J. Astron. Space Sci. 21(4), 303–314 (2004)

MAGNETIC PROPERTIES OF INNER MAGNETOSPHERE DURING GEOMAGNETIC STORMS INFERRED FROM A TSYGANENKO MAGNETIC FIELD MODEL

D.-Y. Lee†, K. C. Kim, C. R. Choi, and H. J. Kim

Department of Astronomy and Space Science, College of Natural Sciences and Institute for Basic Sciences
Chungbuk National University, Cheongju 361-763, Korea

email: dylee@chungbuk.ac.kr

(Received August 12, 2004; Accepted November 12, 2004)

ABSTRACT

In this paper we report some properties of inner magnetospheric structure inferred from the T01_s code, one of the latest magnetospheric models by Tsyganenko. We have constructed three average storms representing moderate, strong, and severe intensity storms using 95 actual storms. The three storms are then modelled by the T01_s code to examine differences in magnetic structure among them. We find that the magnetic structure of intense storms is strikingly different from the normal structure. First, when the storm intensity is large, the field lines anchored at dayside longitudinal sectors become warped tailward to align to the solar wind direction. This is particularly so for the field lines anchored at the longitudinal sectors from postnoon through dusk. Also while for the moderate storm the equatorial magnetic field near geosynchronous altitude is found to be weakest near midnight sector, this depression region expands into even late afternoon sector during the severe storm. Accordingly the field line curvature radius at the equator in the premidnight geosynchronous region becomes unusually small, reaching down to a value less than 500 km. We attribute this strong depression and the dawn-dusk asymmetry to the combined effect from the enhanced tail current and the westward expansion/rotation of the partial ring current.

Keywords: storm, magnetosphere, space weather

1. INTRODUCTION

Major storms are relatively rare events, but because of their dramatic impacts on the magnetosphere and ionosphere, they are the most interesting and relevant phenomenon in space physics. Understanding the inner magnetospheric structure during intense storms is the key to the study of related dynamics such as substorm dipolarization, energetic particle generation, responses to solar wind/IMF variations, etc. Recent simulations (Liemohn et al. 2001, for example) showed that the storm time ring current consists of the classic symmetric ring current and the partial ring current with field-aligned closure currents. Their work showed the buildup of a highly asymmetric dawn-dusk structure and the increasing role

†corresponding author

of the partial ring current for intense storms. From our recent preliminary work based on spacecraft data, we have also found the field depression preferably on the dusk side. Interestingly we sometimes, though not too often, see the magnetic dipolarization even on the duskside, 18 MLT or even earlier, which is not what one can normally expect (Lee & Lyons 2004). Also dispersionless energetic particle flux increase is often observed at dayside sectors in a way similar to normal nightside particle injections (Lee et al. 2004). We believe that all these new features are closely related to the distorted structure of the inner magnetosphere, which therefore warrants the importance of understanding the storm-time magnetic structure in the inner magnetosphere.

The purpose of the present work is to understand differences in the magnetic structure between the storms with different intensity. We use the code T01_s to examine the magnetic structure, which is one of the latest versions of the Tsyganenko models and is suitable for modelling an intense storm.

2. T01_s VERSION OF TSYGANENKO MODEL

The T01_s code used in this study is one of the latest versions of the Tsyganenko geomagnetospheric models. The code is described in detail in recent papers by Tsyganenko and his colleagues (Tsyganenko 2002a,b, Tsyganenko et al. 2003). This is a data-based modeling code that is based on a completely revised mathematical framework, a new set of spacecraft data, and an improved method of parameterizing the external field sources by the solar wind state variables.

The magnetic field within the modeling region is determined by the Earth's main field plus the sum of contributions from major current sources. They are the field of the Chapman-Ferraro current, the ring current field, the tail current field, the fields of the Birkeland currents, and a partial penetration of the IMF inside the model magnetosphere. The magnetospheric boundary is specified using a most recent empirical model (Shue et al. 1998). The code is in modular fashion so that one can choose a particular module(s) to model contributions from a selected current source(s).

One of the new features in the T01_s code, which is absent in earlier data-based models, is that the ring current consists of two components, the SRC (symmetric ring current) and the PRC (partial ring current) with field-aligned closure currents. The inclusion of the PRC contribution enables one to model the dawn-dusk asymmetry that has been observed in recent simulations (Liemohn et al. 2001). Also the T01_s code takes into account the effect due to the preconditioning by the solar wind and IMF state over the previous 1-3 hours from the time of interest.

The T01_s model code is distinguished from the earlier Tsyganenko model codes by its ability to properly represent a strongly disturbed magnetosphere. Earlier models were dominated by much larger amounts of quite time data than intense storm time data, and thus being inappropriate for modeling intense storms. The T01_s is currently the most accurate and useful code particularly in the inner magnetosphere, within $R =\sim 10R_E$, during strongly disturbed periods. Also the nonlinear saturation effect that is seen during

intense storm periods is taken into account in the code.

Modeling by the T01_s code is controlled by Dst index, IMF B_z and B_y, solar wind dynamic pressure P_D as well as two input parameters G2 and G3. The G2 and G3 are the average over the preceding 1 hour interval of the product of solar wind speed and south IMF component, and the product of solar wind particle density, solar wind speed and south IMF component, respectively. They therefore reflect the solar wind condition prior to the time of interest. One may perform parametric studies by varying these six inputs in an arbitrary way, or can take the values from any real storms as inputs. In the present study we have first constructed three representative storms using a number of actual storms with various intensity, and then modelled them by the T01_s code as described below.

3. CALCULATION RESULTS

We have selected 95 storms that occurred in the time period from 1997 to 2002. In this work only the events having the minimum Dst value less than -50 nT have been selected. The solar wind and IMF data corresponding to each selected storm were obtained from observations by several spacecraft, WIND, ACE, GEOTAIL, and IMP-8, when they were located within $50R_E$ from the Sun-earth line. The selected storms were divided into three classes according to the Dst magnitude, moderate, strong, and severe storms. Out of the total 95 storms, 50, 30, and 15 storms correspond to moderate, strong, and severe intensity, respectively. We have obtained three representative storms by averaging the Dst values and the corresponding solar wind and IMF values in each of the three classes. Table 1 shows some of the basic properties of the three storms, the Dst_{min} values, the values of IMF and the dynamic pressure corresponding to the Dst_{min}. The G2 and G3 are parameters needed in T01_s code, the calculation of which requires solar wind and IMF condition over 1 hour prior to the selected time. One can see from the table that, for more intense storm, the IMF becomes more southward and the dynamic pressure becomes stronger.

Also it is interesting that the IMF B_y is positive for all three cases and increases for stronger storms. Our individual storm events have either positive or negative average B_y values, but our three averaged storms happened to correspond to the positive B_y cases. In this work we did not pursue the effect of the B_y polarity or magnitude on the inner magnetospheric structure. However the reader will see below that our main result is convincingly demonstrated in terms of current contributions which are mainly determined by the IMF B_z component rather than B_y.

We have evaluated differences between the three storms using the T01_s code described in the previous section. The values in Table 1 were used as inputs in running the code. The dipole tilt angle was set to zero for convenience. The results are summarized in Figures 1 to 6. The unit of axes in all the figures is the Earth's radius, R_E.

Figure 1 shows field lines for the moderate storm. In all plots the field lines are plotted every 1° in footpoint geocentric latitude beginning with 55° through 70°. Panel (a) shows field lines in xz plane which are anchored at 0° and 180° in longitude. These longitudes correspond to 12 and 24 MLT as demonstrated in panel (h). Not surprisingly, one can

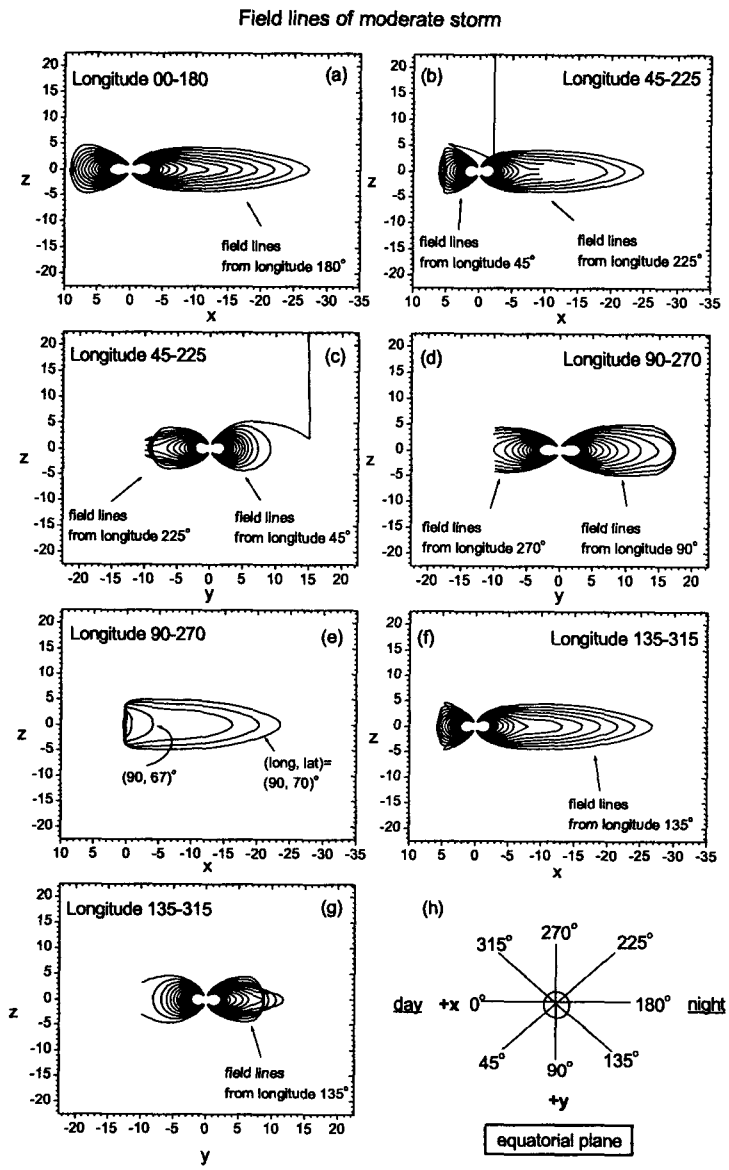

Figure 1. The panels (a)-(g) show the field lines for the moderate storm, being plotted every 1° in footpoint geocentric latitude beginning with 55° through 70°. The different panels represent field lines that are anchored at different geocentric longitudes. The panel (h) demonstrates the correspondence between the geocentric longitude and the MLT region in the equatorial.

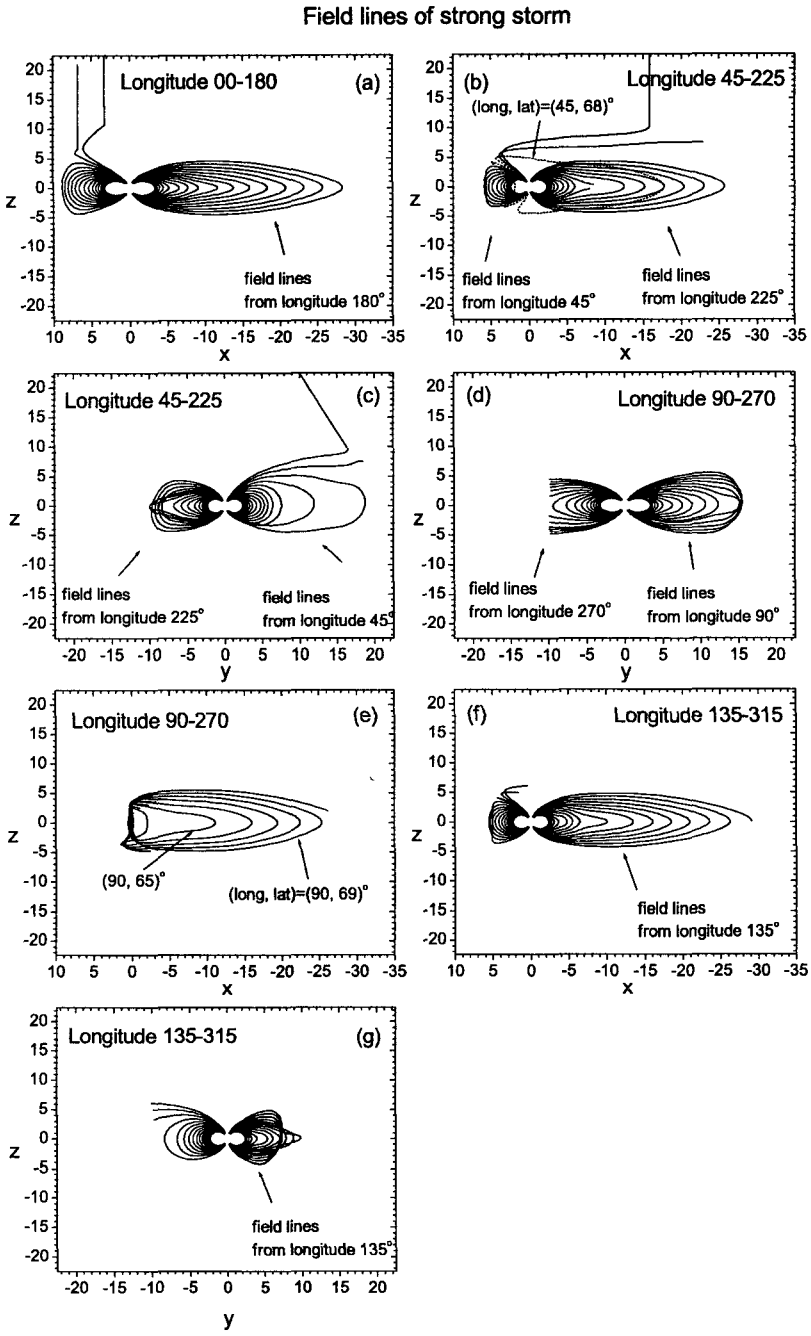

Figure 2. Field lines for the strong storm in the same format as in Figure 1.

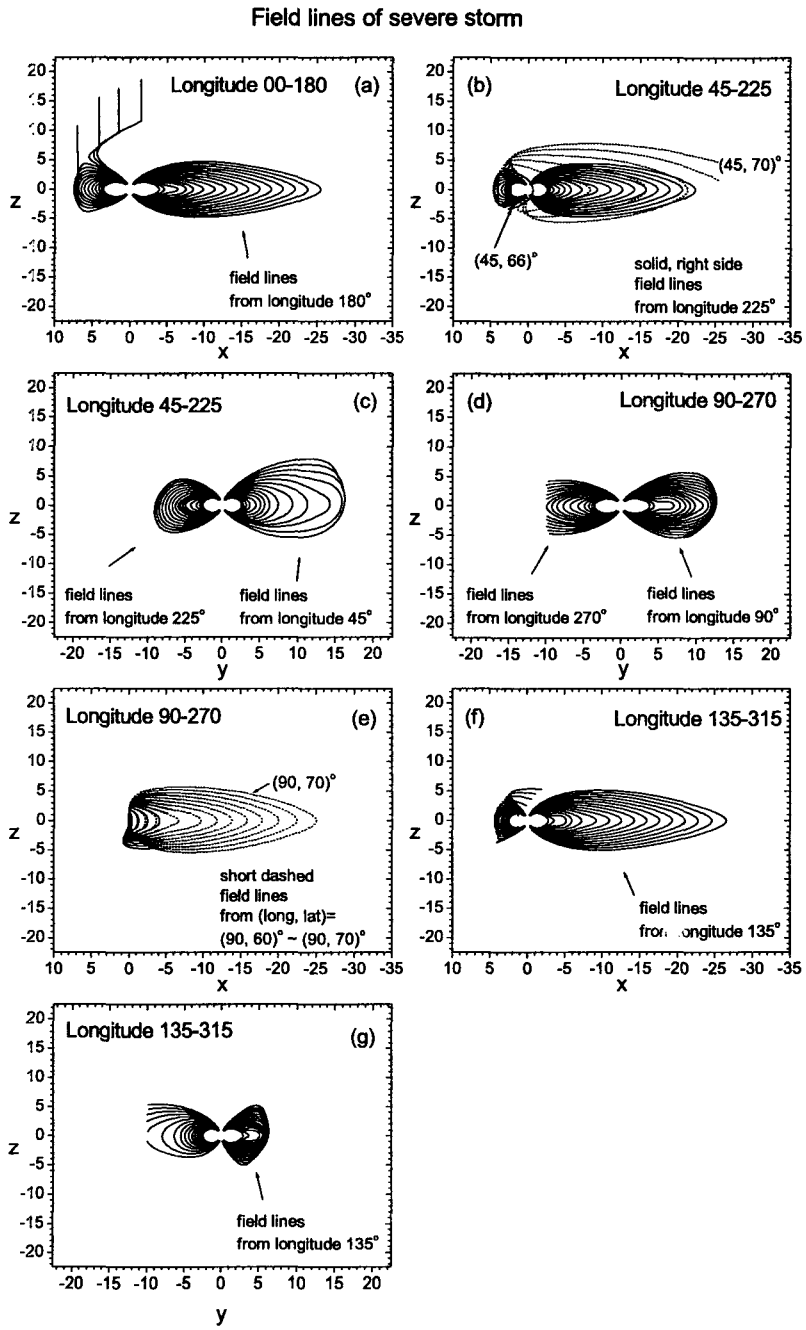

Figure 3. Field lines for the severe storm in the same format as in Figure 1.

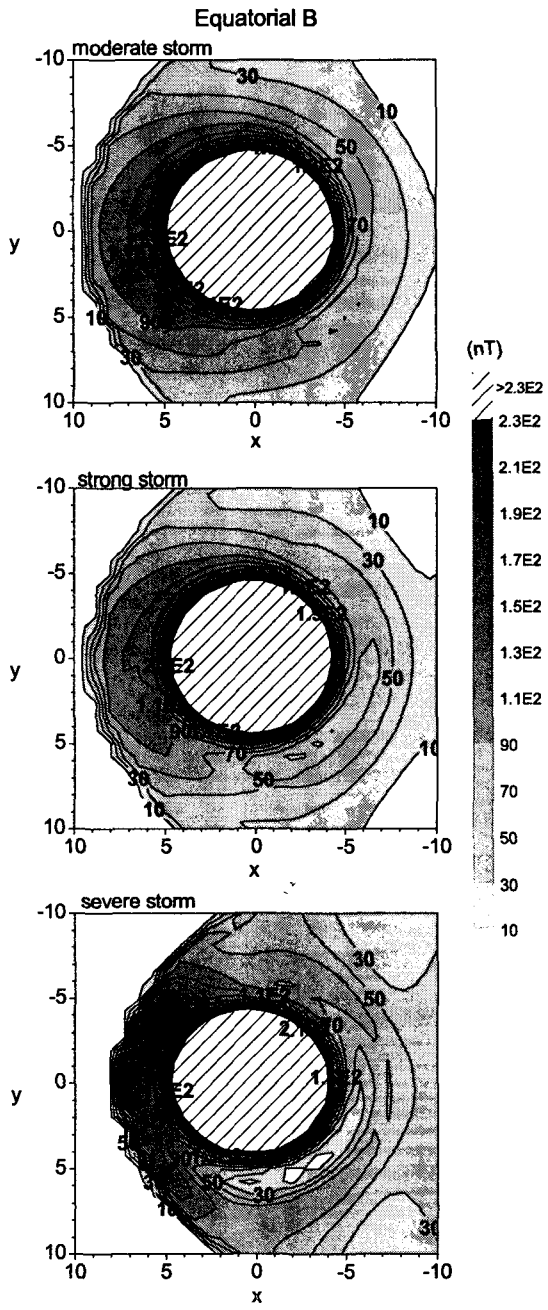

Figure 4. Constant B gray-scale contour at equator for the three storms. The numbers corresponding to each contour represent the magnetic field intensity B in nT. The dipole dominant, high-field, inner region surrounding the Earth is ignored by leaving it as white blank with hatch.

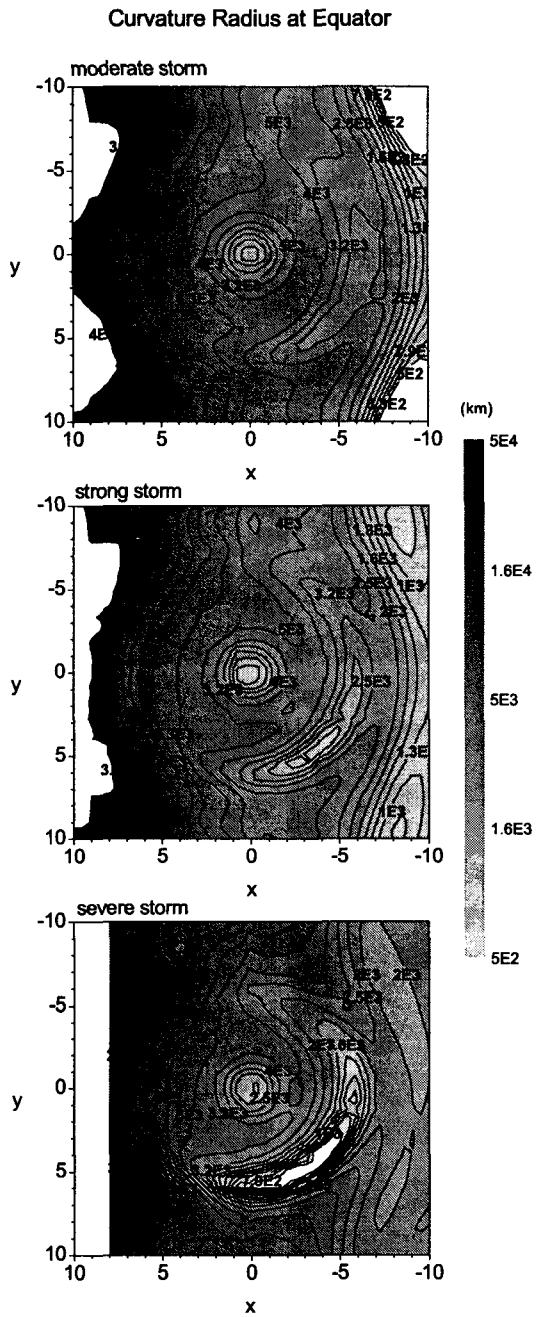

Figure 5. Gray-scale contour of constant Rc (km) at equator for the three storms. The contour plot is in a log scale.

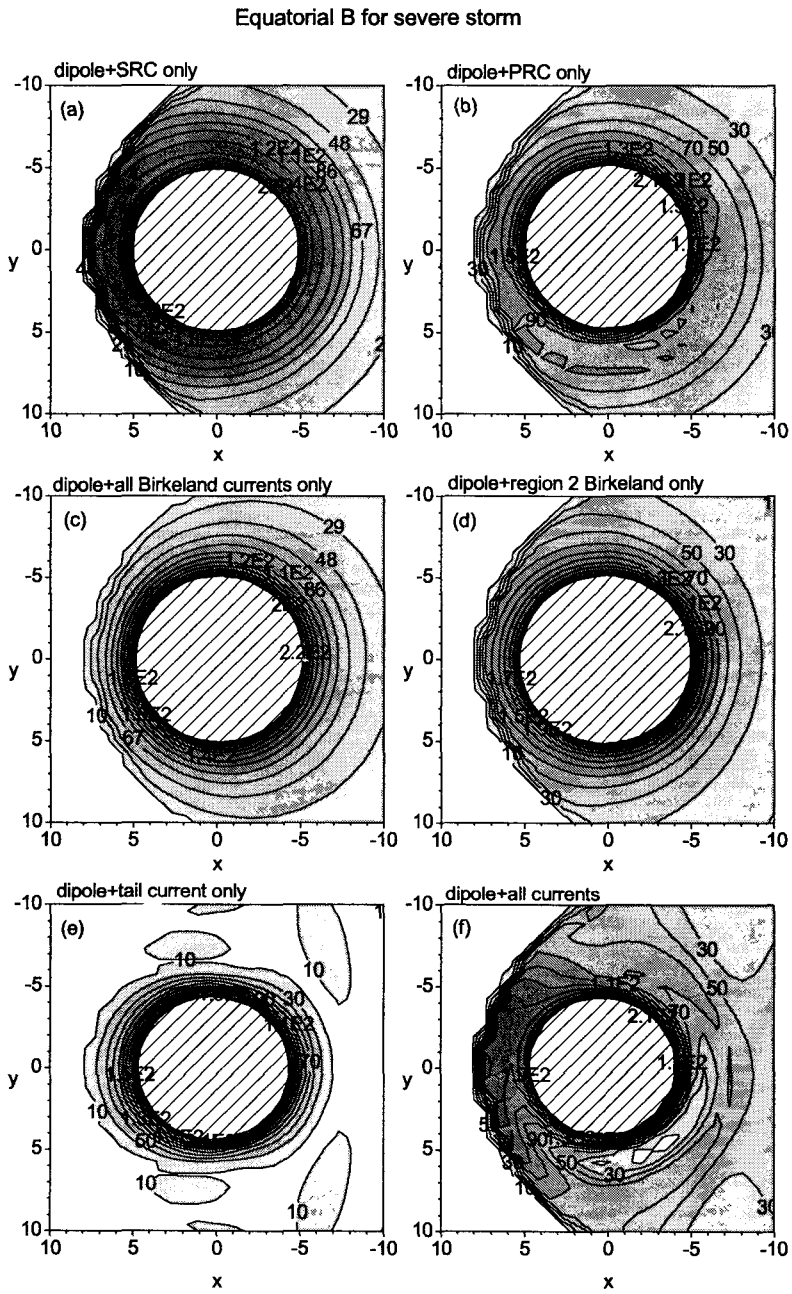

Figure 6. Equatorial constant B contour for different current contributions for the severe storm in the same format as in Figure 4.

see that the field lines on the nightside are stretched in the solar wind direction and on the dayside they are compressed. Panels (b) to (g) show field lines anchored at different longitudinal (or MLT) sectors in the same manner as in Panel (a). Panel (b) shows field lines anchored at 45° and 225° in longitude, being projected in xz plane. The same field lines are projected in yz plane in Panel (c). It is seen that field lines corresponding to 225° (thus being on the nightside) are stretched and tend to be aligned to the x axis, and those corresponding to 45° (in the afternoon sector) are compressed. Field lines shown in Panels (d) and (e) correspond to those anchored at 90° and 270° in longitude. Interestingly, the high latitude (67–70°) field lines anchored in 90° longitudinal sector are stretched and strongly hinged to align themselves parallel to the solar wind direction (–x axis) as shown in Panel (e). This hinging and alignment effect is however not seen in the field lines anchored at 270° longitude in the opposite sector. We will see below that this dawn-dusk asymmetry in the magnetic structure becomes stronger for more intense storms. The field lines shown in Panels (f) and (g) are those anchored at 135° and 315° in longitude, and show stretch on the nightside and compression on the dayside. Also we infer that the outer field lines (at higher latitudes) are more hinged to align to the x axis than the lower latitude field lines.

Field lines for the strong and severe storms are shown in Figures 2 and 3, respectively, in the same format as in Figure 1. The most prominent differences between the three storms can be seen by comparing field lines in Panels (b) and (e) in Figures 1 to 3. From Panel (b) in Figure 2 which is for the strong storm, one can see that some highe latitude field lines anchored at 45° in longitude (i.e. originating from the afternoon side!) are warped back toward the nightside to align to the –x axis. This becomes even more so and more field lines participate in this warped structure for the severe storm, as shown in Panel (b) in Figure 3. Likewise, comparison of Panels (e) in Figures 1–3 demonstrates that, as the storm becomes more intense, the field lines anchored at 90° become more hinged to aligned to –x axis and more field lines participate in this deformation.

Figure 4 shows comparison of equatorial B between the moderate, strong, and severe storms by constant B gray-scale contours. The dipole-dominant, high field, inner region surrounding the Earth is ignored as indicated by white-with-hatch circular region. It is of course not a surprise to see the inward movement of the magnetopause and the consequent enhancement of the near-noon side field strength as the storm becomes more intense (Recall from Table 1 that the more intense storm is associated with a stronger dynamic pressure). It is however striking to see that, for the severe storm, huge depressions of the magnetic field strength are seen in even late afternoon sector through the midnight region near geosynchronous altitude. For the severe storm, the magnetic field strength is depressed down to a value ($\sim$10 nT or even less) that one usually finds in the stretched tail near midnight. It is interesting that the geosynchronous depression region tends to expand in longitude from the nightside toward the late afternoon region as the storm becomes more intense.

The magnetic field depression and the dawn-dusk asymmetry can also be seen in terms of the field line curvature. Figure 5 shows comparison of the curvature radius of the field line at equator R_c between the moderate, strong, and severe storms by constant R_c (in km) gray-scale contours. The most prominent feature is that the smallest R_c region occurs near

Table 1. Three classes of storms used in this study.

storm intensity	Dst_{min}	IMF B_y[a]	IMF B_z[a]	SW P_D[a]	G2[b]	G3[b]
moderate (50)[c]	-76	0.06	-3.23	3.4	13.25	14.66
strong (30)[c]	-117.9	3.78	-7.45	4.56	23.42	29.49
severe (15)[c]	-226.7	7.56	-8.85	13.8	42.7	90.45

[a]IMF in nT, the solar wind dynamic pressure P_D in nPa, all at Dst_{min}.
[b]parameters needed in T01_s code.
[c]number of events used for averaging.

geosynchronous altitude, which expands longitudinally even up to the late afternoon sector from the midnight as the storm becomes more intense. It is seen that, for the severe storm, the R_c is reduced down to less than 500 km near dusk through premidnight sector near geosynchronous altitude, implying an unusual stretch of the field lines.

The field lines are generally made of various current contributions including the SRC and PRC, Birkeland currents, and tail currents. The T01_s code incorporates all the possible current contributions as explained in the previous section. In addition, it is possible to test different current contributions separately. We have done such a test in order to see what current system is mainly responsible for the dawn-dusk asymmetry and the deep depression at geosynchronous altitude which expands even into the late afternoon sector. Figure 6 shows the test result for the severe storm by showing the equatorial B constant contours. Each of the panels is obtained by a combination of selected current contributions: (a) dipole plus SRC only, (b) dipole plus PRC only, (c) dipole plus all kinds of Birkeland currents only, (d) dipole plus region 2 type Birkeland current only, (e) dipole plus tail current only, and (f) dipole plus all kinds of current (this is in fact the same one as the last one in Figure 4). The PRC shown in Panel (b) seems to be the only main source of the dawn-dusk asymmetry. From the Panel (e), we see that the tail current leads to severe depression in a wide range of nightside region. It is most likely that the combination of the tail current and the PRC is the major cause of the dawn-dusk asymmetry and the geosynchronous B depression.

4. DISCUSSION

The stretched field line is a feature that is found normally in near-midnight sectors. Our work showed that, for intense storms, this can be found over a wide MLT regions, way up to dusk side, near geosynchornous orbit. This is probably responsible for the occurrence of dipolarization and energetic particle flux enhancement at sectors far away from midnight. However it remains unclear whether or not one should call this a substorm that is typically limited to MLT sectors near midnight.

The highly stretched and depressed field at dusk side through midnight near geosynchronous orbit during the severe storm implies that the particle dynamics may be quite different from the usual guiding center drift motion encircling the Earth. Remember that we have shown earlier that even the field lines anchored at dayside sectors are warped tailward

to align to the solar wind flow direction. This means a possibility that a proton beginning its westward drift from midnight may follow a non trivial complicated trajectory. In fact our preliminary calculation of test proton trajectories on the basis of the severe storm magnetic field shows non-adiabatic particle motions in the depressed region, much like what is well known from the particle dynamics in the stretched tail geometry. Details of the calculation results will be reported elsewhere.

Being highly distorted, the inner magnetospheric response to a sudden change in the solar wind and IMF may be very different from what is normally expected. For example, what would be the particle reaction in the inner magnetosphere to the sudden increase in the solar wind dynamic pressure during the severe storm? Our current data analysis on the energetic particle response to the solar wind dynamic pressure shows different responses in the particle flux for different IMF B_z conditions. Clearly the state of the inner magnetosphere is first distinguished by IMF B_z polarity, and must be further affected by the strength of the southward IMF. This implies that the particle response must depend on the structure of the inner magnetosphere at and perhaps prior to the time when it is hit by the pressure pulse. This is a subject that we plan to pursue in near future.

ACKNOWLEDGEMENTS: This work was supported by Chungbuk National University Grant in 2004. The *Dst* data were provided by the NASA's NSSDC/Omniweb site. The solar wind and IMF data of WIND, Geotail, and IMP 8 were obtained from NASA's cdaweb site. D.-Y. Lee is grateful to N. Tsyganenko for his help with the T01_s code during the course of this work.

REFERENCES

Lee, D.-Y. & Lyons, L. R. 2004, J. Geophys Res, 109, doi:10.1029/2003JA010076

Lee, D.-Y., Lyons, L. R., & Yumoto, K. 2004, J. Geophys Res, 109, doi:10.1029/2003JA010246

Liemohn, M. W., Kozyra, J. U., Thomsen, M. F., Roeder, J. L., Lu, G., Borovsky, J. E., & Cayton, T. E. 2001, J. Geophys Res, 106, 883

Shue, J.-H., Song, P., Russell, C. T., Steinberg, J. T., Chao, J. K., Zastenker, G., Vaisberg, O. L., Kokubun, S., Singer, H. J., Detman, T. R., & Kawano, H. 1998, J. Geophys Res, 103, 17691

Tsyganenko, N. A. 2002a, J. Geophys Res, 107, 1179, doi:10.1029/2001JA000219

Tsyganenko, N. A. 2002b, J. Geophys Res, 107, 1176, doi:10.1029/2002JA000220

Tsyganenko, N. A., Singer, H. J., & Kasper, J.C. 2003, J. Geophys Res, 108, 1209, doi:10.1029/2002JA009808